QUANTIFICATION AND MODELING OF HYSTERETIC ENERGY DISSIPATION IN RC MEMBERS

M.N. Fardis [1], D. Biskinis[2], S. Grammatikou[3]

[1] *Emeritus Professor, Department of Civil Engineering, University of Patras, Greece, fardis@upatras.gr*

[2] *Instructor and Post-Doctoral Researcher, Department of Civil Engineering, University of Patras, Greece, dbiskinis@upatras.gr*

[3] *Post-Doctoral Researcher, Department of Civil Engineering, University of Patras, Greece, sofgram@upatras.gr*

Abstract

A database of 850 cyclic tests of reinforced concrete (RC) members has been compiled and used to quantify the hysteretic energy dissipation in cyclic loading. The analysis of the data takes into account the shape of the cross-section (circular, rectangular column or wall, members with T- or I-section – including non-rectangular walls, etc), the type and continuity of longitudinal bars (plain or deformed, continuous or with lap-splices, etc), possible wrapping with Fiber-Reinforced Polymer (FRP) and combinations thereof, as well as the amplitude of the cyclic deformations. Hysteretic energy dissipation before yielding – not captured by cyclic force-deformation laws which consider the member as elastic until the yield point – correspond to an average viscous damping ratio around 8.5%, almost independent of the deformation amplitude but depending on the type of member and of its longitudinal reinforcement. A model is proposed for the hysteretic energy dissipation after yielding, in terms of the ductility factor of the cycle, the shape of the cross-section, the continuity and type of the longitudinal bars, the presence or not of FRP wrapping and the likely failure mode - in flexure or in shear. Lap-splicing of longitudinal reinforcement and shear-dominated behavior are found to markedly reduce post-yield energy dissipation. So does wrapping with Fiber-Reinforced Polymer, apparently because it enhances linear behavior. The member's shear-span-to-depth ratio, its dimensionless axial force and longitudinal reinforcement ratio, are also taken into account as parameters, but are found to have secondary importance. Ways are proposed for the application of the findings to describe pinching of the hysteresis loops and/or degradation of unloading stiffness with cycling or other types of effects on residual deformations. The proposed quantification of hysteretic energy dissipation can be incorporated into simple cyclic nonlinear member models for response-history analysis, without sacrificing the convenient and physically appealing use of the secant-to-yield-point stiffness as elastic up to yielding. One way is to reduce the hysteretic energy dissipation after yielding by an amount consistent with the constant damping ratio adopted for the global viscous matrix. The other is to replace the computationally convenient but physically unfounded global viscous matrix, which operates throughout the analysis in parallel with the nonlinear member models, by an element-based separate hysteretic model for the pre-yield range, the secant-to-the yield-point as a skeleton and unloading-reloading rules that reproduce the pre-yield hysteretic energy dissipation.

Keywords: Cyclic tests; Damping; Energy dissipation; Hysteretic models; Reinforced concrete members

1. Introduction

Nonlinear dynamic analysis is widely used today in professional practice for performance-based seismic evaluation of existing concrete structures or, sometimes, of new designs. It can take into account the energy dissipation during the seismic response, which is in essence exclusively hysteretic. To this end, it should use nonlinear force-deformation models for members which represent well the hysteretic energy dissipation. In fact, for an analysis to approximate well the seismic response, member models do not need to trace the experimental behavior in detail; it suffices to represent well the envelope of force-deformation loops and the energy dissipation as a function of the deformation amplitude.

The goal of this paper is to quantify in a simple way the hysteretic energy dissipation in reinforced concrete (RC) members in terms of the inelastic deformation amplitude and of the relevant properties of the member. It does so by compiling a database of cyclic test results on all types of RC members - by far the largest of its kind according to the present knowledge of the authors (see Table 1). All force- (or moment-)deformation loops of each test (digitized in the framework of this work, if not already available in digital form) were used to compute an equivalent viscous damping ratio, ζ, from the energy dissipated in a cycle, E_h, and the elastic deformation energy $E_{el}=F_{max}\delta_{max}/2$, at the cycle's peak force and displacement, as:

$$\zeta = \frac{E_h}{4\pi E_{el}} \tag{1}$$

Several works have fitted empirical formulae relating the peak displacement ductility demand, μ, in a cycle of loading to the equivalent viscous damping ratio from Eq. (1) - e.g. [1-6]. Some of them fitted empirical expressions to a narrow strip of own test results; others, a single curve to a broad cloud of μ-ζ data from literature. Curves fitted to single-source data may be well-defined, but do not reflect other experimental results. Empirical models fitted to a large volume of data from various sources represent better a wider population of tests, but, without an underlying physical model to support the algebraic form chosen, the choice is subjective. Moreover, single μ-ζ curves cannot represent any type of member, regardless of its geometry, materials and other features. As an exception, [6] used as physical μ-ζ model the mathematical relationships between μ and ζ derived from two well-known hysteretic models, as a function of the parameters of these models; it has also fitted expressions for these parameters to test results on RC rectangular or circular columns and rectangular walls, all with continuous deformed (ribbed) bars, in terms of the shear-span-(to-depth)-ratio and the dimensionless axial load of the member. The present work puts the model on a different, type-of-member-based, footing, using a 60% larger database, which covers essentially the full spectrum of member types found in RC buildings, including those with plain (smooth) or lap-spliced bars, shear-critical members, and those retrofitted with wrapping of the end region in a jacket of Fiber Reinforced Polymer (FRP).

Table 1 – The database of cyclic test results

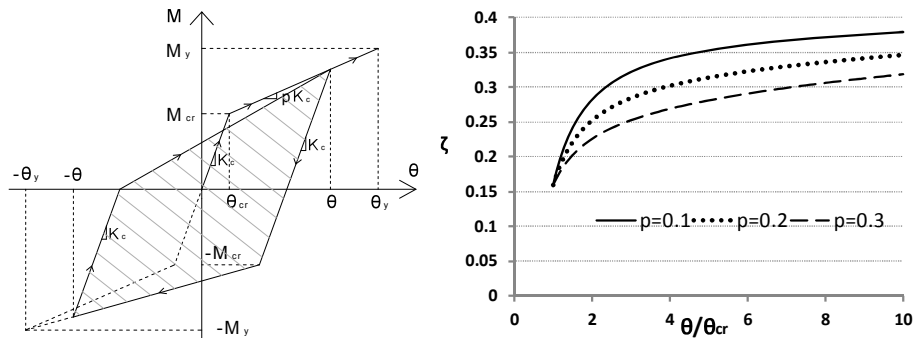| Longitudinal bars	Plain (smooth)				Deformed (ribbed)								
	continuous	lap-spliced		continuous				lap-spliced		continuous			
member	column										wall		pier
section	rectangular				circular		rectangular					nonrectangular	
FRP wrapping	No	Yes	No	Yes	No				Yes	No	Yes	No	
failure mode	flexure					shear		flexure					
number of tests	17	5	11	8	55	93	455	68	55	10	59	10	4
Total tests	41				809								

2

Fig. 1 – Schematic of hysteresis loop that cracks a specimen and equivalent viscous damping

2. Hysteretic energy dissipation before yielding

The single cycle that cracks a member or specimen in positive and negative bending (Fig. 1) dissipates considerable energy. The equivalent damping ratio in a complete cycle with deformation amplitude θ that exceeds for the first time the deformation at cracking, θ_{cr}, is shown in Fig. 1. In this figure the yield moment was fixed as 5-times the cracking moment; parameter p is the "hardening ratio" between cracking and yielding; it has a mean value of 0.18 in rectangular beams/columns or walls, or 0.25 in circular columns.

Examples of pre-yield equivalent damping ratios from specimens in the present database are depicted in Fig. 2. Witness the lack of any clear impact of the magnitude of the peak moment and deformation of the cycle on damping and contrast the high(er) damping values around the estimated cracking moment of the initially uncracked specimens in the figures in the middle and on the right, to the absence of similar effects on the pre-cracked specimens of the figure on the left.
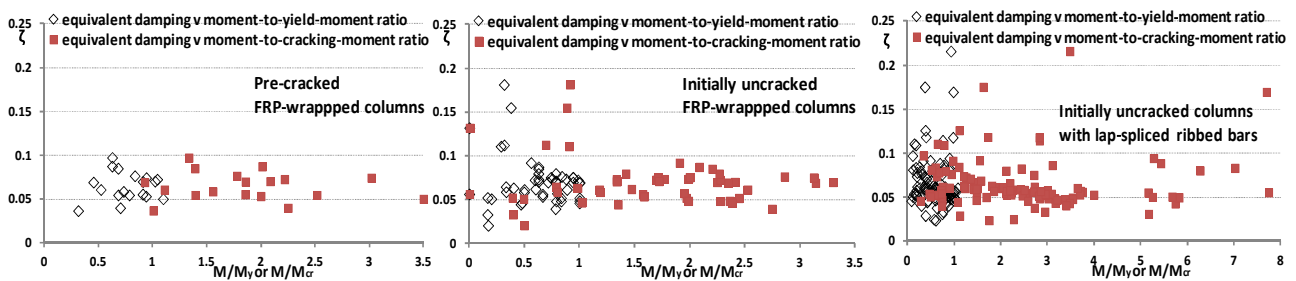

Fig. 2 – Examples of the variation of pre-yield equivalent damping with the amplitude of applied moment

A strong earthquake will most likely find a non-prestressed concrete member already cracked, owing to gravity loads, restraint of thermal or drying shrinkage and/or past earthquakes. So, a simple model is appropriate, which by-passes cracking and has a bilinear force- (or moment-)deformation law in virgin (or monotonic) loading, consisting of a linear-elastic branch to the yield point and a linear post-elastic branch after it, with constant strain hardening ratio p (see Fig. 3). Such a model allows using the tools provided by Structural Dynamics for elastic structures in order to know and control better the key features of the dynamic response. Energy dissipation that takes place before yielding is normally modelled as viscous damping. A default value of 5% of critical is commonly used for viscous damping, as a compromise between steel or prestressed concrete components, which have less pre-yield damping, and RC or masonry ones, which have more. However, the cyclic tests of concrete members suggest that, even with the cycle that cracks the member in positive and/or negative bending omitted, the energy dissipation before yielding corresponds to an amplitude-independent viscous damping ratio markedly higher than the default value of 5%. Average values per member category and overall are listed in Table 2. The systematic differences between member categories notwithstanding, the values in Table 2 point to an average pre-yield equivalent damping ratio of 8.5% for members with deformed (ribbed) longitudinal bars, or of 8% for those with plain (smooth) bars.

3

Table 2 – Average equivalent damping ratio before yielding in member categories of the database

| Longitudinal bars	Plain (smooth)				Deformed (ribbed)						
	continuous		lap-spliced		continuous				lap-spliced		continuous
member/section	rectangular columns				circular columns	rectangular columns					walls/piers
FRP wraps	No	Yes	No	Yes	No			Yes	No	Yes	No
failure mode	flexure					shear	flexure				
equivalent damping	0.106	0.06	0.077	0.06	0.074	0.073	0.094	0.082	0.058	0.048	0.128
average	0.076				0.08						
weighted average	0.084				0.089						
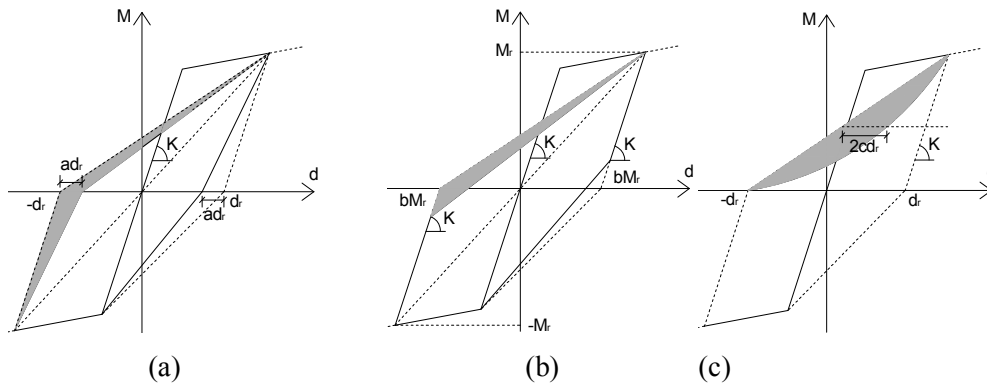
Fig. 3 – Simple hysteretic force-deformation models and loss in energy dissipation with respect to the "reference hysteresis model" (shown with a dotted line) due to: (a) degradation of unloading stiffness (modified Takeda model); (b) "early reload"; (c) "pinching" with parabolic reloading.

3. Hysteretic energy dissipation after yielding

Before yielding the equivalent viscous damping ratio, ζ, is independent of the amplitude of deformation. After yielding, it increases with increasing ductility ratio μ (: ratio of peak deformation in a cycle to the deformation at yielding). It is expressed in this work as a fraction of the equivalent viscous damping ratio of a "reference hysteresis model" (shown in Fig. 3 with a dashed line) which has:

- a bilinear primary (or virgin, or monotonic) loading curve, consisting of an elastic branch to the yield point and a post-elastic branch with constant hardening ratio p, serving as skeleton of the peaks of full unload-reload loops;
- linear unloading from the peak point on the post-elastic branch of the primary curve with the elastic stiffness (i.e., parallel to the elastic primary branch) until the horizontal axis is reached at a residual deformation d_r;
- linear, peak-oriented reloading, i.e., from the residual deformation after unloading, straight to the peak point ever reached before on the post-elastic branch in the current direction of reloading.

The "reference hysteresis model" gives an "equivalent" viscous damping ratio, ζ_o, equal to:

$$\zeta_o = (1 - p)/\pi(1 - 1/\mu) \tag{2}$$

4

The same dependence on p and μ is retained for the equivalent viscous damping ratio, ζ, derived from the experimental hysteresis loops of the database; ζ is taken to be a fraction $(1-\lambda)$ of ζ_o, with λ called "loss in energy dissipation":

$$\zeta = (1 - \lambda)\zeta_o = (1 - \lambda)(1 - p)/\pi(1 - 1/\mu) \tag{3}$$

The global viscous damping which is used to model hysteretic energy dissipation in the members themselves, as well as the energy dissipated in components which are not included in the structural model (infill walls, other non-structural elements, or structural ones that are not part of the lateral-load-resisting system) or are taken as rigid (e.g., floor diaphragms), is retained throughout the nonlinear analysis of the response, i.e., after the members enter the post-yield range. So, if the hysteretic model used for members accounts fully for the energy they dissipate, the energy dissipated by the concurrently operating viscous damping is counted twice. To avoid such double-counting, the parameters of the member's post-yield hysteretic model should be set so that the model dissipates the balance between the energy corresponding to its deformation state (i.e., to the current value of its ductility factor) and the energy dissipated by global viscous damping, the damping ratio of which is denoted by ζ_v. In other words, Eq. (3) becomes:

$$\zeta = \zeta_v + (1 - \lambda_v)\zeta_o = \zeta_v + (1 - \lambda_v)(1 - p)/\pi(1 - 1/\mu) \tag{4}$$

So, the value of λ becomes a function of the viscous damping ratio, ζ_v, used in the analysis of the system (hence the subscript v). Accordingly, the mean values of the loss in post-yield energy dissipation relative to the "reference hysteretic model", denoted by $\lambda_{v,o}$ and listed in Table 4, have been determined from the database for three values of ζ_v:

a. 8.5%, i.e., the overall average value found in Section 2 to be representative of the pre-yield hysteretic energy dissipation in RC members, if they are modelled as linear-elastic until they yield;
b. 5%, i.e., the commonly used, default value of global viscous damping ratio; and
c. 0%; as the value appropriate for a model with hysteretic energy dissipation before yielding of the member itself, which is "switched-off", once the member (or relevant part thereof) yields.

The last column of Table 4 gives the overall average values of the loss in post-yield energy dissipation over the entire database.

Table 4 – Mean loss in post-yield energy dissipation relative to "reference hysteretic model", $\lambda_{v,o}$, for the member categories in the database

Longitudinal bars	Plain (smooth)		Deformed (ribbed)								
	continuous	lap-spliced	continuous				lap-spliced	continuous		
member/section	rectangular columns		circular	rectangular columns				walls/piers		All members
FRP wraps	No	Yes	No	Yes	No		Yes	No	Yes	No	
failure mode	flexure				shear		flexure				
$\lambda_{v,o}$ for $\zeta_v = 0\%$	0.297	0.430	0.412	0.535	0.253	0.415	0.171	0.329	0.371	0.436	0.222	0.262
$\lambda_{v,o}$ for $\zeta_v = 5\%$	0.519	0.687	0.651	0.740	0.482	0.607	0.398	0.563	0.603	0.687	0.466	0.489
$\lambda_{v,o}$ for $\zeta_v = 8.5\%$	0.622	0.775	0.785	0.826	0.584	0.724	0.513	0.686	0.717	0.797	0.632	0.6

Extensive correlation analyses carried out to identify variables which systematically affect post-yield hysteretic damping came up with the following choice:

- the shear-span(-to-depth)-ratio L_s/h
- the axial load ratio, $\nu = N/A_c f_c$
- the total longitudinal steel ratio, ρ_{tot}

with L_s denoting the shear span (moment-to-shear-ratio) at the yielding end of the member, h the depth of the cross section and A_c its area, and N the axial load, with compression taken as positive. These three variables were found to have the most consistent effect on the loss in energy dissipation across all categories of members - with some exceptions, though. Other variables of general applicability, such as the transverse reinforcement ratio, were found to be significantly correlated in the database with one or two of the three variables above. The transverse reinforcement ratio, for example:

- is positively correlated with the axial load ratio, because column specimens with heavy axial load were usually provided with substantial confinement reinforcement;
- has higher values in flexure-controlled specimens than in those critical in shear - which were kept in different member categories, anyway;
- was positively correlated with the longitudinal reinforcement ratio, as they were both on the low side in specimens designed to reflect defficient, non-conforming construction, and on the high side in those meant to represent well-detailed, conforming members.

The inherently large scatter of the loss in energy dissipation obscures any systematic effect of key variables on member categories with relatively small number of specimens. This was the case of the lap length in specimens with lap-spliced longitudinal bars, or of the mechanical ratio of FRP in the relevant special categories.

Last, but not least, variables which are considered as important thanks to their effect on ultimate resistance and deformation capacity, may not be so relevant over the entire spectrum of deformation amplitudes associated with energy dissipation.

Mean values of the loss in energy dissipation, $\lambda_{v,o}$, listed in Table 4 correspond to the mean value of the variables which affect post-yield hysteretic damping over the relevant member category, $(L_s/h)_o$, ν_o and $\rho_{tot,o}$. These mean values are listed in Table 5. A linear model is adopted for the loss in energy dissipation at other values of these variables:

$$\lambda_v = \lambda_{v,o} + a_{Ls/h,v}(L_s/h - (L_s/h)_o) + a_{v,v}(\nu - \nu_o) + a_{\rho tot,v}(\rho_{tot} - \rho_{tot,o}) \tag{5}$$

The values of the slope parameters, $a_{Ls/h,v}$, $a_{v,v}(\nu - \nu_o)$, $a_{\rho tot,v}$, estimated from the database are listed in Table 6. They apply alongside the mean values of the loss and of the three variables affecting it which are listed in Tables 4 and 5, respectively.

Table 5 – Mean value of variables affecting post-yield hysteretic damping in member categories of database

Longitudinal bars	Plain (smooth)				Deformed (ribbed)						
	continuous		lap-spliced		continuous				lap-spliced		continuous
member/section	rectangular columns				circ. columns	rectangular columns					walls/piers
FRP wraps	No	Yes	No	Yes	No			Yes	No	Yes	No
failure mode	flexure					shear		flexure			
mean shear span ratio $(L_s/h)_o$	4.63	6.4	4.98	6.18	3.83	2.49	3.97	4.31	4.73	4.61	2.05
mean axial load ratio, ν_o	0.155	0.384	0.24	0.412	0.137	0.156	0.17	0.297	0.141	0.282	0.14
mean long. steel ratio, $\rho_{tot,o}$ %	1.23	1.03	0.95	1.05	2.29	2.22	2.16	1.63	1.39	0.89	0.35

6

Table 6 – "Slope" of regression of loss in post-yield energy dissipation relative to "reference hysteretic model" on variables affecting post-yield hysteretic dissipation and standard error of the regression

slope with respect to:	shear span ratio, $a_{Ls/h,v}$	axial load ratio, $a_{v,v}$	steel ratio, $a_{\rho tot,v}$	standard error
For $\zeta_v = 0\%$	0.0187 (-)	0.12	0.05 (-)	0.23 (90.5% of total)
For $\zeta_v = 5\%$	0.0165 (-)	0.17	0.055 (-)	0.23 (91% of total)
For $\zeta_v = 8.5\%$	0.018 (-)	0.08	0.04 (-)	0.225 (91% of total)

With Eq. (5) written in the format of Eq. (6), the values of the "intercept", a_v, are given in Table 7.

$$\lambda_v = a_v + a_{Ls/h,v}L_s/h + a_{v,v}\nu + a_{\rho tot,v}\rho_{tot} \tag{6}$$

Eqs. (5) or (6), used with the values of parameters and the mean values of variables given in Tables 4 to 6, leave a residual with respect to the individual loss values of each test of the database. The standard deviation of the residual ("standard error" of the regression), listed in the last column of Table 6, is high, over 90% of that of the individual data with respect to the overall mean values of loss, listed at the last column of Table 4.

Table 7 –Loss in post-yield energy dissipation relative to "reference hysteretic model" at zero values of the variables affecting post-yield hysteretic dissipation (intercept of linear regression equation) per member category in the database

Longitudinal bars	Plain (smooth)		Deformed (ribbed)						
	continuous	lap-spliced	continuous			lap-spliced	continuous		
member/section	rectangular columns		circ. columns	rectangular columns					walls/piers
FRP wraps	No	Yes	No	Yes	No		Yes	No	Yes	No
failure mode	flexure				shear		flexure			
For $\zeta_v = 0\%$	0.427	0.556	0.524	0.654	0.424	0.555	0.334	0.456	0.512	0.533	0.261
For $\zeta_v = 5\%$	0.637	0.783	0.744	0.000	0.648	0.745	0.554	0.674	0.734	0.764	0.495
For $\zeta_v = 8.5\%$	0.739	0.898	0.891	0.000	0.729	0.841	0.652	0.802	0.843	0.891	0.670

In view of the failure of Eqs. (5) or (6), used together with the values inTables 4 to 6, to explain a major part of the scatter of the data, a simplification is suggested here. It is shown in Table 8 and comprises the following:

- the loss in energy dissipation is constant in each category of members in the database; any dependence on the shear span, axial load and steel ratios is neglected;
- the starting point are the 5% viscous damping values of loss for the five reference member types (shown in Table 8 in bold):
  - $\lambda_v = 0.4$, for the flexure-controlled rectangular columns with continuous deformed bars;
  - $\lambda_v = 0.45$, for the flexure-controlled walls with continuous deformed bars;
  - $\lambda_v = 0.5$, for the flexure-controlled circular columns with continuous deformed bars;
  - $\lambda_v = 0.5$, for the flexure-controlled rectangular columns with continuous plain bars;
  - $\lambda_v = 0.6$, for the shear-controlled rectangular columns with continuous deformed bars;

7

- the values of loss for the five reference member types, to be applied alongside the two other values of damping, are obtained from the 5%-damping values as follows (see entries in italics in Table 8):
  - for ζ_v = 0%, by reducing the 5%-damping values of the normally better performing and conforming types of member (namely, the flexure-controlled rectangular or circular columns and the walls), by 0.25 and those of the normally more deficient and poorly performing types (namely the flexure-controlled rectangular columns with continuous plain bars and the shear-controlled rectangular ones with deformed bars) by 0.2;
  - for ζ_v = 8.5%, by increasing the 5%-damping values for walls by 0.2, and those of the four other reference member types by 0.1;
- the values of loss for rectangular columns with lap-spliced vertical bars or FRP wrapping may be obtained from those applying for continuous bars and no FRP wrapping, by adding 0.15 for columns with plain bars or 0.2 for those with deformed bars;
- in members with lap-spliced bars and FRP wrapping, the values of loss in energy dissipation may be obtained by adding 0.25 to the values applying for continuous bars and no FRP wrapping for columns with plain bars, or 0.3 for those with deformed bars.

Despite the major difference of the suggested simplification from the more "accurate" estimation using Eqs. (5) and (6) and Tables 4 to 7, its impact on accuracy is minor. As shown in the last column of Table 8, the already high values of "standard error" increase very little.

The simplified rules are general enough to be extended to types of members not included in the analysis, owing to the very small number of pertinent tests in the literature (e.g., members with plain bars or shear-dominated ones other than rectangular columns).

If a value of the viscous damping ratio other than 0, 5 or 8.5% is used for the anlysis of the system alongside a hysteresis model of the members which is linear-elastic till yielding, linear interpolation may be applied, to the values in Tables 4 and 6 to 8.

Table 8– Rounded values of the loss in post-yield energy dissipation relative to "reference hysteretic model" for the member categories, to be used neglecting the impact of any other variable

Longitudinal bars	Plain (smooth)				Deformed (ribbed)							Standard error (% of the total)
	continuous		lap-spliced		Continuous				lap-spliced	continuous		
member/section	rectangular columns				circular columns	rectangular columns					walls/piers	
FRP wraps	No	Yes	No	Yes	No	No	No	Yes	No	Yes	No	
failure mode	flexure					shear	flexure					
For ζ_v = 0%	*0.3*	0.45	0.45	0.55	*0.25*	*0.4*	*0.15*	0.35	0.35	0.45	*0.2*	0.24 (93.5%)
For ζ_v = 5%	**0.5**	0.65	0.65	0.75	**0.5**	**0.6**	**0.4**	0.6	0.6	0.7	**0.45**	0.23 (91%)
For ζ_v = 8.5%	*0.6*	0.75	0.75	0.85	*0.6*	*0.7*	*0.5*	0.7	0.7	0.8	*0.65*	0.235 (95%)

4. Application for nonlinear response history analysis

Loss in energy dissipation with respect to the "reference hysteresis model" may take place in various ways and combinations thereof. Three typical ones are shown in Fig. 3:

a) degrading unloading stiffness, as in the modified Takeda model [7, 8], controlled by unloading parameter *a* (Fig. 3(a));

8

b) "early reload" (or "aborted unloading") in Fig. 3(b), controlled by unloading parameter *b*;

c) "pinching" of the loop, chosen in Fig. 3(c) to take the form of parabolic reloading which produces a linear increase of the reloading stiffness with increasing force, controlled by pinching parameter *c*.

In Fig. 3 the ratio of the shaded area to the triangular one enclosed by the chord connecting the positive to the negative peak on the primary branches and by the single unload-reload path between these peaks in the "reference hysteresis model", is the loss in energy dissipation. So, if the three models in Fig. 3 are used, alone or in combination, a value of the "loss in energy dissipation" λ is related to the parameters of the three models as follows:

$$a + b + 4c/3 = \lambda \qquad (7)$$

To see the impact of the details of the hysteresis model for given loss in energy dissipation, a SDoF system comprising a column fixed against rotation at top and bottom, but free to translate at the top, has been modeled using options (a) to (c) above and in Fig. 3 and subjected to nonlinear response-history analysis. The moment-chord rotation loops obtained using the three options are shown in Fig. 4 to have serious but not systematic differences; nevertheless, the drift histories depicted in Fig. 5 are not so different. Therefore, for given loss in energy dissipation with respect to the "reference hysteresis model", the exact shape of the hysteresis loops may be considered to play a certain role for the global response, but not a persistent or dominant one.
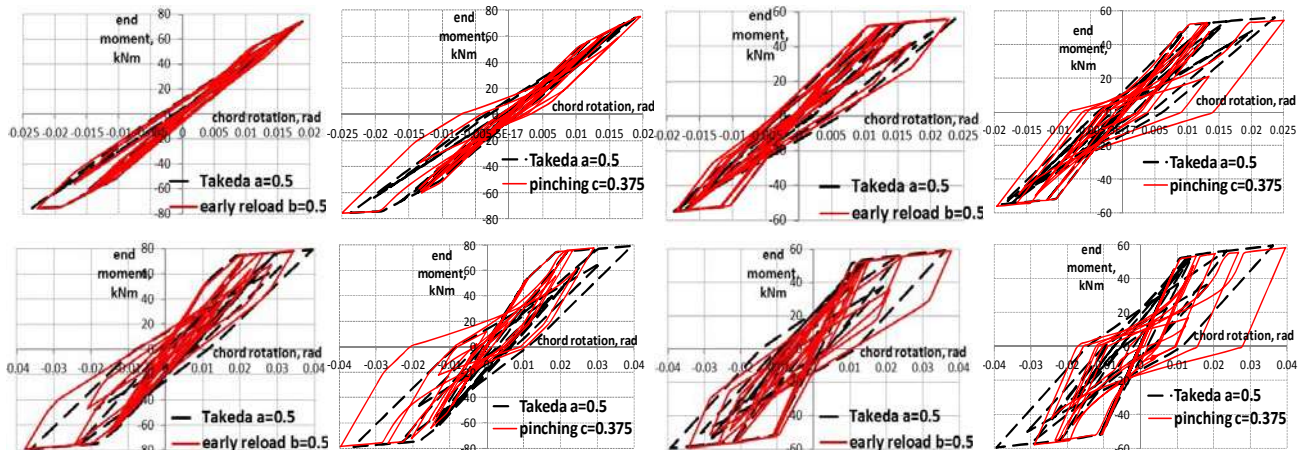

Fig. 4 - Moment-chord rotation loops at the ends of a SDoF column for 50% loss in energy dissipation with respect to the "reference hysteresis model", due to degradation of unloading stiffness in the modified Takeda, early reload or pinching models, for the Herzegnovi record scaled to a PGA of (*top*): 0.12g; (*bottom*): 0.24g.
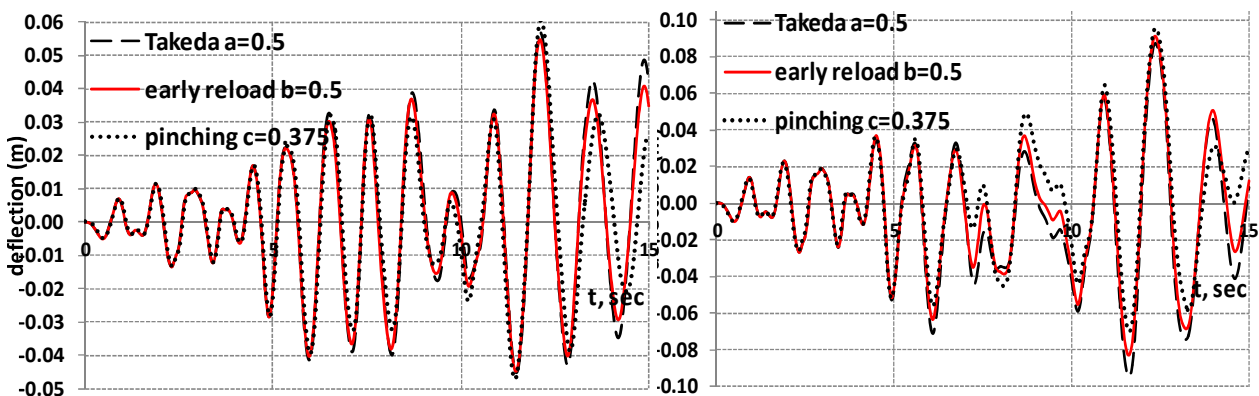

Fig. 5 - Drift-histories from the same analyses as in Fig. 4 for excitation scaled to (*left*) 0.12g; (*right*) 0.24g

9

An alternative to using viscous damping to take into account hysteretic energy dissipation before yielding (and reducing hysteretic energy dissipation according to Eq. (4), to compensate for the operation of viscous damping in the post-elastic range) is to abolish completely viscous damping and model pre-yield energy dissipation through the special element proposed in [6]. That element combines hysteretic energy dissipation before yielding with linear-elastic behavior under virgin loading. The element is linear-elastic in virgin loading until the yield point and uses the linear elastic branch as skeleton curve for cyclic loading before yielding. However, it dissipates energy in a hysteretic way during cycles of loading before yielding. The dissipated energy, E_h, in a full cycle from a point on the linear-elastic branch back to the same point, is equivalent to a viscous damping ratio according to Eq. (1). The value of this ratio is taken to be constant until yielding and denoted by ζ_v. The results of this work concerning hysteretic energy dissipation before yielding may be applied to determine the value of ζ_v.

A nonlinear rotational spring with this pre-yield hysteretic behavior should be added to each member end, in series with the elastic member itself. That spring is active before flexural yielding at the corresponding member end and switched off when the corresponding end section of the member yields; it is then replaced by the nonlinear spring featuring the post-yield hysteresis rules. As long as the spring is active (i.e., till yielding at the corresponding end) it is assigned a fraction f_{el} of the elastic flexibility L/EI of the member at that end, at the expense of the flexibility of the elastic member.
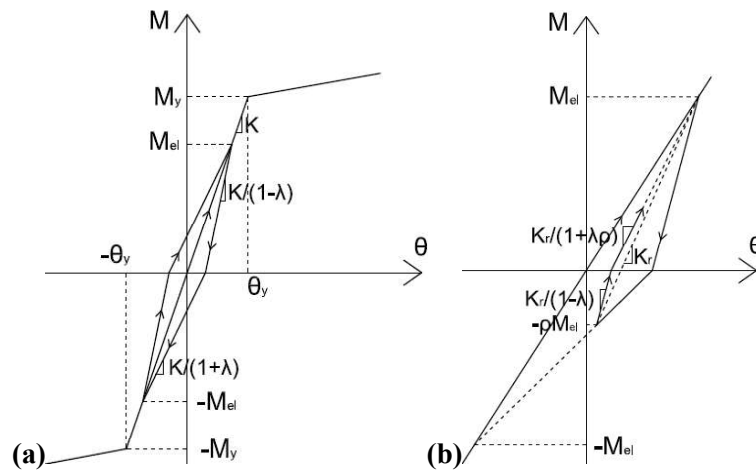

Fig. 6 - (a) Hysteresis model dissipating energy equivalent to damping ratio $\zeta=\lambda/\pi$ in symmetric pre-yield cycles; (c) model's intermediate unloading rule [6].

The rules of the model are the following (Fig. 6):

1. Unloading from the linear-elastic branch is linear, leading to a residual deformation equal to a fraction $\pi\zeta_v/f_{el}$ of the deformation at reversal on the linear-elastic branch. As the spring accounts for a fraction f_{el} of the total deformation of the member at the end considered, this residual deformation gives hysteretic energy dissipation in the member equivalent to the target viscous damping ζ_v. For $\pi\zeta_o/f_{el}$ to be less than 1.0, the value of f_{el} should meet Eq. (9):

$$f_{el} > \pi\zeta_v \qquad (9)$$

This gives a positive unloading stiffness equal to:

$$K_{un} = K_o/(1- \pi\zeta_o/f_{el}) \qquad (10)$$

where K_o is the elastic stiffness of the nonlinear spring.

2. If unloading continues beyond the residual deformation in 1 above, it turns into (re)loading in the opposite direction. No matter whether this is the first time loading in that direction takes place or not, (re)loading heads towards the mirror point of the point of reversal on the virgin loading curve that led to

10

the unloading in 1. If loading reverses at this mirror point and the new unloading continues into reloading in the original direction after reaching a residual deformation equal to $\pi\zeta_v/f_{el}$ times the deformation at this last reversal, Eq. (1) gives viscous damping ratio equal to ζ_v.

3. Upon a reversal on an unloading branch before the horizontal axis is crossed, the reloading that follows traces the unloading branch towards the last point of reversal on the skeleton curve. If there is a new reversal before the skeleton curve is reached, the unloading branch is traced in the opposite direction towards the residual deformation in 1 above.

4. Unloading from a point on a reloading branch takes place with the unloading stiffness given by Eq. (10). If there is a reversal before the horizontal axis is reached, rule 3 applies. After reaching the horizontal axis, unloading turns into re-loading in the opposite direction and heads toward the extreme past point on the skeleton curve in the current direction of loading.

5. After reloading reaches the most extreme past point on the skeleton curve in either direction or its mirror image, it turns into virgin loading along the linear-elastic branch.

5. Conclusions

A database of 850 cyclic tests of reinforced concrete members has been compiled and used to quantify the hysteretic energy dissipation in cyclic loading. The data have been categorized in 13 categories according to Table 1, depending on the shape of the cross-section (circular, rectangular column or wall, nonrectangular wall or hollow rectangular pier), the type and continuity of longitudinal bars (plain or deformed, continuous or with lap-splices), the likely failure mode (in flexure or in shear), wrapping or not with FRP and combinations thereof. Because they give very similar results, rectangular and nonrectangular walls and hollow rectangular piers can be grouped together, reducing the categories by two, to 11.

Hysteretic energy dissipation before yielding is markedly higher than commonly assumed in analysis; it is equivalent to a viscous damping ratio of 8% to 9%, on average. It is essentially independent of the deformation amplitude but depends on the type of member and the type and continuity of its longitudinal reinforcement. It often peaks around the moment and deformation which cause cracking at the end section.

A model is proposed for the hysteretic energy dissipation after yielding, in terms of the ductility factor of the cycle. It is expressed on the basis of the energy dissipated by a "reference hysteresis model", which unloads to the horizontal axis parallel to the elastic branch to the yield point, and reloads thereafter towards the extreme past point on the post-yield, hardening branch in the direction of reloading. The reduction in energy dissipation relative to that of the "reference hysteresis model" is quantified on the basis of the experimental database. It is found to depend strongly on the discrete member category, but marginally on the continuous variables found to affect post-yield energy dissipation the most: the shear-span(-to-depth)-ratio, the axial load - normalized to the compressive strength of the concrete section - and the total longitudinal steel ratio. The linear expressions in terms of these variables which are fitted to the experimental data of the database offer very little advantage over a simpler approach which takes into account the member category alone, and indeed, in a very simplified way.

Lap-splicing of the longitudinal reinforcement and shear-dominated behavior are found to markedly reduce post-yield energy dissipation. So does wrapping with Fiber-Reinforced Polymer, apparently because it enhances linear behavior.

Ways proposed for the application of the findings can describe pinching of the hysteresis loops and/or degradation of unloading stiffness with cycling or other types of effects on residual deformations.

The proposed quantification of hysteretic energy dissipation can be incorporated into simple cyclic nonlinear member models for response-history analysis, without sacrificing the convenient and physically appealing use of the secant-to-yield-point stiffness as elastic stiffness until yielding. One way is to reduce the hysteretic energy dissipation after yielding by an amount consistent with the constant damping ratio adopted for the global viscous matrix. The other is to replace the computationally convenient but physically unfounded

global viscous matrix, which operates throughout the analysis in parallel with the nonlinear member models, by an element-based separate hysteretic model for the pre-yield range, which uses the secant-to-the yield-point as a skeleton and has unloading-reloading rules that reproduce the pre-yield hysteretic energy dissipation.

6 Acknowledgements

7. References

[1] Shibata A, Sozen MA (1976): Substitute-structure method for seismic design in R/C. *Journal of the Structural Division, ASCE* **102** (ST1), 1-18.

[2] Blandon CA, Priestley MJN (2005): Equivalent viscous damping equations for direct displacement based design. *Journal of Earthquake Engineering* **9** (SI 2), 257-278

[3] Elmenshawi A, Brown T (2010): Hysteretic energy and damping capacity of flexural elements constructed with different concrete strengths. *Engineering Structures* **32**, 297–305

[4] Rodrigues H, Varum H, Arêde A, Costa A (2012): A comparative analysis of energy dissipation and equivalent viscous damping of RC columns subjected to uniaxial and biaxial loading *Engineering Structures* **35**, 149-164

[5] Zhang Y, Gong J, Zhang Q, Han S (2012): Equivalent damping ratio model of flexure-shear critical RC columns. *Engineering Structures* **130**, 52-66

[6] Grammatikou S, Fardis MN, Biskinis DE (2019): Energy dissipation models for RC members and structures. *Earthquake Engineering and Structural Dynamics* **48**(3), 287-305

[7] Takeda T, Sozen MA, Nielsen NN (1970): RC response to simulated earthquakes. *Journal of the Structural Division, ASCE* **96**, 2557-2573.

[8] Otani S (1974): Inelastic analysis of RC frame structures *Journal of the Structural Division*, *ASCE* **100**, 1433-1449